Eur. Phys. J. B **36**, 349–357 (2003)
DOI: 10.1140/epjb/e2003-00353-6

THE EUROPEAN PHYSICAL JOURNAL B

Light scattering and dielectric manifestations of secondary relaxations in molecular glassformers

A. Brodin[1], R. Bergman[2], J. Mattsson[2,a], and E.A. Rössler[1,b]

[1] Experimentalphysik II, Universität Bayreuth, 95440 Bayreuth, Germany
[2] Department of Applied Physics, Chalmers University of Technology, 41296 Göteborg, Sweden

Received 21 July 2003
Published online 23 December 2003 –

Abstract. Photon correlation data of the molecular glass-forming materials 2-picoline, dimethylphthalate (DMP) and salol are compared with their dielectric loss spectra in the time-frequency range where the dielectric data reveal secondary relaxations. Slow secondary relaxation processes in molecular liquids are commonly studied by dielectric spectroscopy (DS) and, based on such studies, believed to be characteristics of the deeply super-cooled liquid state. However, there has been no direct experimental evidence that they are similarly detected by other experimental techniques. In the present study, we experimentally address this question for the anisotropic (depolarized) light scattering (LS). In the first approximation, DS and LS probe the same molecular reorientation dynamics, and therefore are expected to provide qualitatively similar spectra. We find however that this is not the case, namely i) the magnitude of the slow secondary relaxations is much less in LS than in DS data, which is the opposite to expectations; ii) the shape of the relaxation spectrum is qualitatively different, concerning both the main and secondary processes. We discuss possible sources of these differences in the context of related data from the literature.

PACS. 64.70.Pf Glass transitions – 77.22.Gm Dielectric loss and relaxation – 78.35.+c Brillouin and Rayleigh scattering other light scattering

Introduction

Structural relaxation of super-cooled liquids, albeit a complex phenomenon, exhibits features that are believed to be universal. Decay of structural fluctuations starts at picosecond times as oscillation dephasing and proceeds through intermediate, or "secondary" relaxation processes, to the ultimate decay towards equilibrium known as the α-relaxation. The dynamic structural variable in this context usually refers to the particle density, and thus its spectrum is the dynamic structure factor. The latter is however not easily accessible experimentally. Moreover, there are other variables pertaining to the structure of molecular liquids, notably the molecular orientations. Different variables of dense fluids are however strongly coupled, and therefore the dynamics are related and the spectra usually similar. It is a well-established experimental fact that, at moderate degrees of super-cooling, the dynamic susceptibility spectra obtained by different experimental techniques, such as dielectric absorption, quasi-elastic incoherent neutron and light scattering, indeed exhibit the same characteristic features. These universal characteristics include the α-relaxation stretching, the existence of a characteristic susceptibility minimum, and a power-law shape of the susceptibility above the minimum. In fact it is an important prediction of the Mode Coupling Theory (MCT) [1] that the susceptibility minimum has a universal shape. Based on this, it has been a common practice to perform MCT and phenomenological analyses of different experimental data without much concern regarding the nature of the dynamic variables probed in these experiments.

As the super-cooling proceeds and the average relaxation time $\langle\tau_\alpha\rangle$ becomes 10^{-8} s and longer, the time window between the α-relaxation and fast picosecond dynamics widens and additional, secondary relaxation features become visible. In the case of flexible molecules, such as linear polymers, intramolecular motions may give rise to secondary relaxations. However even in simple liquids of rigid molecules, the susceptibility spectra show characteristic changes. The most useful spectroscopic technique to study these intermediate relaxation phenomena is Dielectric Spectroscopy (DS), owing to the enormous μHz-GHz frequency range offered by the technique. Discussions of the relaxation susceptibility spectra of deeply super-cooled glass-formers are therefore mostly based on broadband DS data. Such studies suggest two additional generic features,

[a] *Presently at*: DEAS and Physics Department, Harvard University, Cambridge, MA 02138, USA
[b] e-mail: ernst.roessler@uni-bayreuth.de

appearing in the dielectric loss spectra of simple molecular glass-formers on approaching the glass transition temperature T_g: the so-called excess wing of the α-peak and a slow, or Johari-Goldstein (JG) β-relaxation with a temperature activated relaxation rate in the kHz-MHz range [2]. Consequently, a classification of simple glass-formers into type A and B has been suggested, according to whether they show an excess wing or a JG process, respectively [3]. Conclusions on generality or classifications are however incomplete as long as they are based on results of a single experimental technique. It is therefore desirable to experimentally investigate whether the typical secondary relaxation spectral patterns observed by DS are similarly seen in other spectroscopic data. There is indeed experimental evidence that NMR spin-lattice relaxation, NMR lineshape analyses, and anisotropic (depolarized) light scattering (LS) results of simple organic glass-formers are consistent with the assumption that the corresponding dynamic susceptibilities are similar to the dielectric loss spectra. For instance, Adichtchev et al. [4] show that their LS spectra of picoline (type A glass-former), obtained by interferometric spectroscopy in the GHz range, are compatible with the assumption that the (experimentally inaccessible) kHz-MHz spectra resemble the dielectric ones. Likewise, Blochowicz et al. in their systematic study of dielectric *versus* NMR spin-lattice relaxation [5] were able to quantitatively reproduce the temperature dependence of the spin-lattice relaxation time in glycerol by approximating the relevant spectral density at the Larmor frequency with the corresponding dielectric spectral density. However, to our knowledge there is no direct spectroscopic evidence of the similarity of different susceptibilities. Indeed, the relevant kHz frequency window is not accessible to light scattering spectroscopy in the frequency domain. It is however accessible to Photon Correlation Spectroscopy (PCS), which is a time domain light scattering method [6]. It was demonstrated that PCS allows to directly detect secondary relaxations in certain polymers [7–9] and B_2O_3 glass [10]. On the other hand, Comez et al. [11] report that their LS data of a super-cooled epoxy resin showed no sign of the secondary process despite the fact that the latter was detected by DS with almost the same amplitude as the main relaxation. One thus concludes that LS and dielectric spectra may be qualitatively different. It is therefore desirable to extend such investigations and include other systems, in particular those of simple and preferably rigid molecules, where the results can be interpreted more easily. However, there are to our knowledge no such studies of simple molecular glass-formers. This observation motivated us to conduct the present study and experimentally address the question of the relaxation patterns of several molecular liquids, as detected by LS and dielectric spectroscopy, specifically targeting secondary relaxation features.

In the context of the present paper, we will distinguish three different time/frequency scales. Figure 1 shows a typical normalized relaxation function of a molecular liquid close to its glass transition temperature and illustrates three relaxation regimes: i) the main, or α-relaxation in

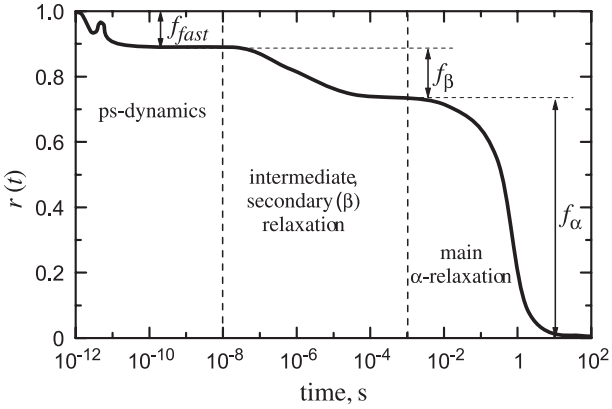

Fig. 1. Schematic three-step relaxation function.

Hz frequency range for $T \sim T_g$; ii) an intermediate, or secondary (β) relaxation that occurs on the kHz-MHz frequency scale and includes the excess wing and/or JG processes (we will not explicitly distinguish them for most of the following discussion); iii) fast picosecond, or ps-dynamics in the GHz-THz frequency range, which includes vibrational dynamics and any fast relaxation processes that are outside of the accessible time/frequency range of our experiments. f_{fast}, f_β, and f_α denote the strengths of the processes.

Theoretical background

The theoretical problem of the relaxation patterns in anisotropic (depolarized) LS versus dielectric spectra of molecular liquids can be discussed in terms of the molecular orientational correlation functions:

$$\phi_l(t) = \langle P_l(\cos\theta_t)\rangle \tag{1}$$

where $\langle \dots \rangle$ denotes an ensemble average in a uniform, isotropic (rotationally invariant) liquid, $\phi_l(t)$ is the normalized ($\phi_l(0) = 1$) orientational correlation function of rank l, $P_l(x)$ the Legendre polynomial of rank l, and θ_t the angle through which the molecular axis rotates in time t. One then shows [12] that, under simplifying assumptions mentioned below, the correlation functions in LS and DS are

$$\phi_{LS}(t) = \left\langle (1/2)(3\cos^2(\theta_t) - 1)\right\rangle = \phi_2(t),$$
$$\phi_{DS}(t) = \langle \cos(\theta_t)\rangle = \phi_1(t). \tag{2}$$

Before we proceed to analyzing equation (2), we explicitly mention the underlying assumptions, as we will have to question them later in the discussion: i) interaction induced effects are relatively weak; ii) intermolecular orientational correlations are neglected; iii) the molecular polarizability tensor is axisymmetric. One expects, then, that the differences or similarities of $\phi_{\rm LS}(t)$ and $\phi_{\rm DS}(t)$ can be traced to the relation between $\phi_2(t)$ and $\phi_1(t)$. There is however no general relation between the orientational correlation functions of different rank, as they depend in

a non-trivial way on the underlying stochastic process. Therefore, in order to make comparisons, one needs additional assumptions about the reorientation process.

The following reasoning partly follows that of reference [12]; the results are however somewhat different. Let us examine $\phi_l(t)$ at short times $t \ll \langle\tau_\alpha\rangle$. The molecules are then bound to the cages formed by their surrounding and oscillate (librate) in the transient potential wells, whose lifetime is $\sim \langle\tau_\alpha\rangle$ and thus much longer, in the super-cooled state, than the characteristic ps time of the molecular vibrations. One can then argue that, at short times, the rotation angle θ_t of the molecules that make statistically significant contributions to equations (2) is small, $\theta_t \ll 1$. One can further assume that, even at longer than ps times (but still $t \ll \langle\tau_\alpha\rangle$), an average molecule's rotation angle is small. Indeed, rotations through large angles imply significant loss of the orientational correlation, and therefore only occur at $t \sim \langle\tau_\alpha\rangle$. Conversely, such rotations require corresponding cage rearrangements, i.e. the cage relaxation that occurs on the time scale of τ_α. Assuming thus $\theta_t \ll 1$, one expands $P_l(\cos\theta_t)$ in equation (1) to the leading order in θ_t, $P_l(\cos\theta_t) \approx 1 - \frac{1}{4}l(l+1)\theta_t^2$, and notes that for $l = 1, 2$ and for angles as large as $\theta = \pi/6$ this is accurate to better than 10%. Then $\phi_l(t) \approx 1 - \frac{1}{4}l(l+1)\langle\theta_t^2\rangle$. In order to now compare the dielectric and LS response, i.e. $l = 1$ and 2, we need to make an additional assumption that the molecular electric dipole is aligned with the symmetry axis of the polarizability tensor, so that θ refers to the orientation of the same molecular axis for $l = 1$ and 2. Alternatively, one can assume that molecular reorientations are isotropic, and therefore the correlation functions independent of the choice of molecular axis (in which case one does not need to assume axial symmetry of the polarizability). Recalling equations (2), we finally get, for short times $t \ll \langle\tau_\alpha\rangle$,

$$1 - \phi_{\mathrm{LS}}(t) = 3(1 - \phi_{\mathrm{DS}}(t)). \tag{3}$$

Equation (3) tells us that the initial parts of the correlation functions $\phi_{\mathrm{LS}}(t)$ and $\phi_{\mathrm{DS}}(t)$ are essentially identical in shape until the beginning of the main α-relaxation; the decay of $\phi_{\mathrm{LS}}(t)$ occurs however with three times larger magnitude than $\phi_{\mathrm{DS}}(t)$. Equation (3) thus implies that

$$\begin{aligned} f_{fast}^{\mathrm{LS}} &= 3f_{fast}^{\mathrm{DS}}, \\ f_{\beta}^{\mathrm{LS}} &= 3f_{\beta}^{\mathrm{DS}} \end{aligned} \tag{4}$$

(the last result was also obtained by Blochowicz et al. [5]). The normalized susceptibility $\chi(t)$ equals, by fluctuation-dissipation theorem, the time derivative of $-\phi(t)$, which leads to

$$\chi_{LS}(t) = 3\chi_{DS}(t). \tag{5}$$

Considering now the susceptibility in frequency domain $\chi''(\omega) = \int_0^\infty \chi(t)\sin\omega t\, dt$ and noting that its spectrum at high frequencies $\omega > 1/\tau$ is mostly determined by the dynamics at short times $0 < t < \tau$, we write down the frequency-domain version of equation (5):

$$\chi''_{LS}(\omega) = 3\chi''_{DS}(\omega)\,, \text{ for } \omega \gg 1/\tau_\alpha\,, \tag{6}$$

which suggests that at frequencies significantly above the α-peak maximum, the LS spectrum is expected to resemble the DS one and be 3 times more intense.

We would like to reiterate that the preceding discussion only concerns the initial part of the correlation functions, i.e. relatively short times, and that a more general relation between the orientational correlation functions of different rank can only be established along with a model for the orientational dynamics itself, such as the rotational diffusion or rotational jump models [6]. In fact, the reasoning leading to equations (3, 5), and (6) would fail even at short times if the molecules performed large magnitude orientational jumps. Let us therefore examine the large-angle jump supposition in its physically unrealistic extreme, i.e. the random jump model [13]. In this model, a molecule rests for a (random, in general) waiting time, and then instantly reorients by an arbitrary angle, so that the orientational correlation is completely lost in one single step, irrespectively of the rank of the correlation function. The correlation functions and the corresponding spectra are then independent of l, so that equations (2) yield $\phi_{\mathrm{LS}}(t) = \phi_{\mathrm{DS}}(t)$.

Experimental

For the present study, we have chosen three representative molecular liquids: 2-picoline, salol, and dimethylphthalate (DMP). They have been studied in the past by dielectric spectroscopy and are known to display secondary relaxation features of different kinds, namely an excess wing in picoline [4], a JG process in DMP [14], and an intermediate type of a relaxation feature in salol [15,16]. Salol and picoline are rigid molecules (except for rotation of the methyl group of picoline), and therefore do not possess internal degrees of freedom that may interfere with their relaxation dynamics. These liquids can be vacuum-distilled, and they give rise to strong depolarized light scattering, both properties being highly desirable for optical spectroscopic studies.

2-picoline (98%), salol (99%), and DMP (96+%) were purchased from Sigma-Aldrich. We determined the calorimetric (onset) T_g's of the liquids as 133, 218, and 195 K, respectively.

DS measurements were carried out at Chalmers University with a Novocontrol Alpha-S Dielectric Analyzer, using a standard 20 mm diameter parallel plate capacitor cell with 100 μm Si spacers. For a data consistency check, we also measured dielectric relaxation spectra at Bayreuth University using a Schlumberger SI 1260 impedance analyzer with a broad band impedance converter by Novocontrol and a spacer-free sample cell. The two data sets were in good agreement.

Samples of 2-picoline, salol, and DMP for light scattering were vacuum-distilled directly into cylindrical 10 mm diameter glass cells that were flame sealed under vacuum. A sample cell, mounted in an Oxford coldfinger cryostat, was illuminated by a 100 mW 532 nm focused laser beam from a Coherent Verdi V2 frequency-doubled Nd:YVO_4 single mode laser. Scattered light was collected in 90° HH

(horizontal-horizontal, depolarized) scattering geometry, coupled into a single mode optical fiber, and fed through a beam-splitter into two fast photomultipliers. The photomultipliers' outputs were cross-correlated by an ALV-5000/FAST Multiple Tau digital correlator, which provides up to 288 correlation channels with lag times from 0 to 3.2×10^3 s and an initial time resolution of 12.5 ns. The PCS data of each sample were collected at ∼15 temperatures in the range $\sim T_g$ to $T_g + 30$ K, typically for 2 hrs at each temperature. The output of the correlator is the normalized count rate (intensity) autocorrelation function $g_2(t) = \langle I(0)I(t)\rangle / \langle I\rangle^2$ which, in the present case of homodyne detection, is related to the normalized electric field autocorrelation function $g_1(t)$ through $g_2(t) = 1 + ag_1^2(t)$, where $a \leq 1$ is an instrumental coherence factor [6]. The coherence factor is related to the number of simultaneously detected coherence areas [6] and, in the case of single mode fiber light collection, is expected to be 1. We measured a using a polystyrene latex standard and found that $a = 1$ to experimental precision. Since we collected the depolarized component of the scattered light, $g_1(t)$ has to be identified with the normalized LS correlation function $\phi_{\rm LS}(t)$ discussed above. Therefore, our measured PCS data $g_2(t)$ are related to $\phi_{\rm LS}(t)$ as follows:

$$\phi^2_{\rm LS}(t) = g_2(t) - 1. \tag{7}$$

In the following we present measured PCS data as $\phi^2_{\rm LS}(t)$, i.e. without the unit background.

To transform the data between the time and frequency representations, we used the single sided cosine transform:

$$S(\omega) = \int_0^\infty F(t)\cos\omega t\, dt\,,$$
$$F(t) = \frac{2}{\pi}\int_0^\infty S(\omega)\cos\omega t\, d\omega, \tag{8}$$

where ω is the angular frequency. This convention of real Fourier transform is commonly used in the dielectric spectroscopy literature [17] (note that the area of the normalized spectrum $S(\omega)$ is $\pi/2$). Numerical transforms of discretely sampled data were done using linear interpolation between the sampled points.

Results and analyses

Figure 2a shows PCS data of DMP at several selected temperatures that demonstrate the characteristic slowing down of α-relaxation with decreasing temperature. It is seen that, at the shortest accessible times $\sim 10^{-8}$ s, the *measured* initial values $\phi_0 = \phi_{\rm LS}(\sim 10^{-8}\,{\rm s})$ are less than 1. In particular, at $T = 199$ K the correlation function $\phi^2_{\rm LS}(t)$ starts from $\phi_0^2 \approx 0.86$, see Figure 2b, and exhibits little decay until the main α-relaxation sets in at ∼10 ms. ϕ_0 is less than one due to the dynamics that are significantly faster than the time resolution $\Delta\tau = 12.5$ ns of the correlator, so that $1-\phi_0$ is the strength of these dynamics, i.e. their integrated spectral density. Assuming that most of the intermediate relaxations are slower than 12.5 ns, the strength

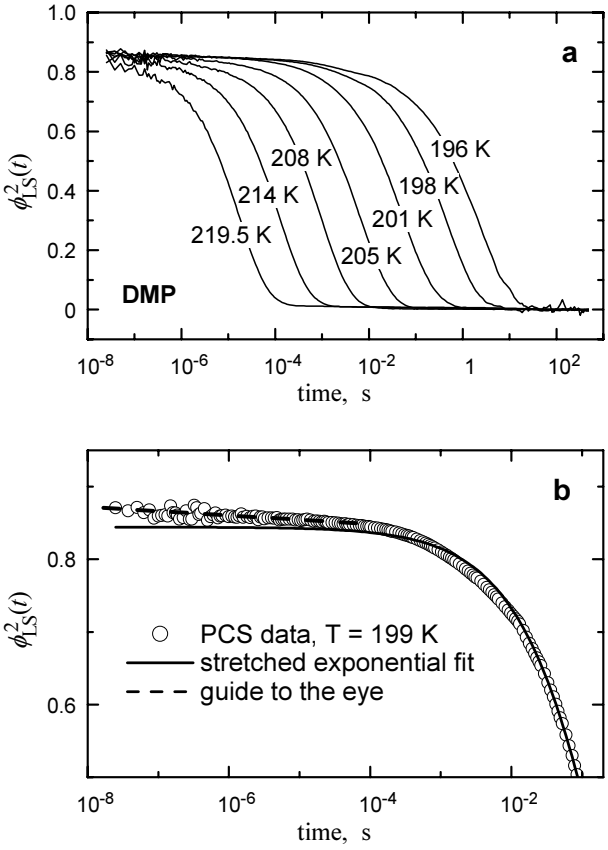

Fig. 2. (a) PCS data $\phi^2_{\rm LS}(t)$ of DMP at selected temperatures. (b) Initial part of $\phi^2_{\rm LS}(t)$ at 199 K with a stretched exponential fit.

of the ps-dynamics in the LS data is thus $f^{LS}_{fast} \approx 1 - \phi_0$. The main α-relaxation is usually well described by the Kohlrausch-Williams-Watts (KWW) stretched exponential function $\phi_\alpha(t) = f_\alpha e^{-(t/\tau_K)^{\beta_K}}$ with an initial value $f_\alpha < 1$ that we will identify, for the purpose of this work, with the α-relaxation strength (cf. Fig. 1). We note that at the lowest temperatures of all the studied systems, KWW fits were not completely satisfactory, indeed as one expects if there are additional, secondary relaxation dynamics preceding the main relaxation. This is illustrated in Figure 2b, which shows that it is exactly the initial short-time part of the correlation function that deviates from the stretched exponential. The experimental correlation function clearly decays within $10^{-8} < t < 10^{-4}$ s, where the stretched exponential stays practically constant. We therefore conclude that the initial decay of correlation is due to intermediate relaxation processes. Figure 3 displays PCS data of DMP (open circles) at a temperature of 198 K, which is just above the calorimetric $T_g = 195$ K. To separate the main α- from intermediate relaxations, we fit the PCS data in Figure 3 to the KWW function only in the range of the main decay, arbitrarily defined to be from 0.7 to 0.1 (using other similar limits, say 0.6 to 0.05, does not change the result to any significant degree, as long as the data at short times are not included). The result is the solid line, which clearly does not fit the data at

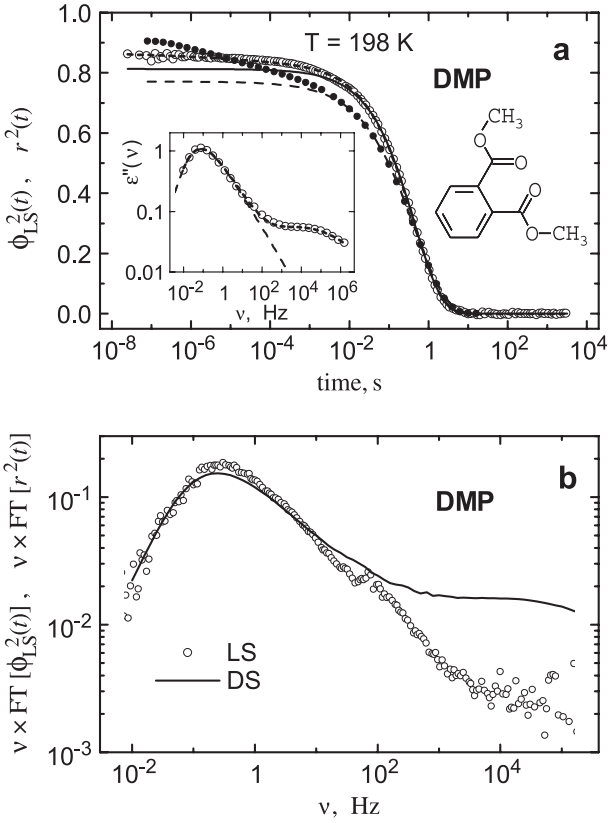

Fig. 3. (a) PCS data $\phi^2_{\rm LS}(t)$ (○) and squared normalized dielectric relaxation function $r^2(t)$ (●) of DMP at 198 K. Solid and broken lines are KWW fits of $\phi^2_{\rm LS}(t)$ and $r^2(t)$, respectively; short-dashed line is an extended fit of $\phi^2_{\rm LS}(t)$ (see text for details). Inset: Dielectric loss spectrum $\epsilon''(f)$ with the same KWW fit as above (broken line) and an extended fit that describes also the β-process (short-dashed line). (b) $\phi^2_{\rm LS}(t)$ and $r^2(t)$ transformed into the frequency domain.

$t < 10^{-2}$ s, so that the KWW description is inadequate, as already noted. The short-time data points all fall above the fit, the difference being just the secondary relaxation dynamics, whose strength is $f^{\rm LS}_\beta = \phi_0 - f^{\rm LS}_\alpha$. In order to learn whether this intermediate relaxation can be identified with the JG β-relaxation process at kHz frequencies, seen in the dielectric loss spectrum (inset in Fig. 3), we proceed to directly compare the time domain PCS and the frequency domain dielectric data, which is only possible if both are presented in the same (time or frequency) representation. We first convert $\epsilon''(\nu)$ into the normalized dielectric relaxation function

$$r(t) = \frac{2}{\pi(\epsilon_0 - \epsilon_\infty)} \int_0^\infty \frac{\epsilon''(\omega)}{\omega} \cos\omega t \, dt \qquad (9)$$

and note that $r(t) = \phi_{\rm DS}(t)$ $(t > 0)$ by fluctuation-dissipation theorem. We assumed $\epsilon_0 \approx \epsilon'(0.01\,{\rm Hz})$ and $\epsilon_\infty \approx n^2$, where n is the refractive index at optical frequencies. The latter was estimated as $n \approx n_D^{20\ ^\circ{\rm C}} = 1.5150$ (supplier's data), neglecting its weak dispersion and temperature dependence. In Figure 3a we plot $r^2(t)$ (dots) for comparisons with the PCS data. It is seen that its value at the shortest times $r_0^2 = r^2(10^{-7}\,{\rm s}) \approx 0.9$, while $\phi_0^2 \approx 0.85$. As for the LS data, $f^{\rm DS}_{fast} \approx 1 - r_0$ is the magnitude of ps-dynamics, which is therefore different for LS and DS, $f^{\rm LS}_{fast} > f^{\rm DS}_{fast}$. This is qualitatively in accord with equations (4). However, the strength of the secondary relaxation $f^{\rm LS}_\beta = \phi_0 - f^{\rm LS}_\alpha$ and $f^{\rm DS}_\beta = r_0 - f^{\rm DS}_\alpha$ exhibits the opposite trend, $f^{\rm LS}_\beta < f^{\rm DS}_\beta$. This is quite evident without any fitting: $r^2(t)$ decays considerably between 10^{-7} and 10^{-4} s, while $\phi^2_{\rm LS}(t)$ by comparison stays almost unchanged. We therefore conclude that the secondary relaxation process in DMP is much more pronounced in the DS than in LS data, and that this is in conflict with equations (4).

Now we turn to comparing the data of Figure 3a in the frequency representation. One way would be to find $\chi''_{\rm LS}(\nu)$ from $\phi_{\rm LS}(t)$ and compare it with $\epsilon''(\nu)$, but taking the square root of $\phi^2_{\rm LS}$ amplifies the noise. We therefore transform $\phi^2_{\rm LS}$ directly into the corresponding "susceptibility", which is proportional to the autoconvolution of the spectral density, $\omega\times$ FT $[\phi^2_{\rm LS}] = \omega S(\omega) \otimes S(\omega)$. $r^2(t)$ is transformed accordingly. The peak of the so obtained "susceptibility" is shifted by a factor of $\sim$2 up in frequency, but otherwise is almost identical to the true susceptibility. The results are shown in Figure 3b (a minor feature of the LS data around 100 Hz is an interference at twice the ac line frequency). One immediately observes a marked difference between the spectral shapes of Figure 3b. Yet the tail of the LS spectrum above 1 kHz is clearly reminiscent of the secondary relaxation feature around 10^4 Hz of the DS data, albeit with significantly reduced intensity. We therefore proceed to a quantitative analysis, intending to learn whether the excess contribution in the light scattering data can indeed be identified with the intermediate relaxation process seen in the inset in Figure 3a. Fitting both LS and DS data to the same model would answer the question. We chose the stretched exponential function as the model for the α-process, $\phi_\alpha(t) = e^{-(t/\tau_K)^{\beta_K}}$, and an additional $\phi_\beta(t)$ that was defined in relaxation time domain by a symmetric normalized distribution, following Blochowicz et al. [18]:

$$G_\beta(\ln\tau) = \frac{2a}{\pi}\left(\left(\frac{\tau}{\tau_\beta}\right)^a + \left(\frac{\tau}{\tau_\beta}\right)^{-a}\right)^{-1}, \qquad (10)$$

from which $\phi_\beta(t)$ is obtained by Laplace transform

$$\phi_\beta(t) = \int_{-\infty}^{\infty} G_\beta(\ln\tau)\, e^{-t/\tau}\, d\ln\tau \qquad (11)$$

that was calculated numerically on a 12 per decade grid spanning 80 decades. $\phi_\alpha(t)$ and $\phi_\beta(t)$ were then combined using the multiplicative, or Williams-Watts ansatz:

$$\phi_{\alpha\beta}(t) = \big(f_\alpha + f_\beta\phi_\beta(t)\big)\,\phi_\alpha(t)\,. \qquad (12)$$

The resulting function thus does not include the ps-dynamics. It has 6 parameters, f_α, τ_K and β_K of the α-peak, f_β, τ_β and a of the β-peak. We first fitted the dielectric loss spectra to a Fourier transform of equation (12) (a sample fit is shown by a short-dashed line

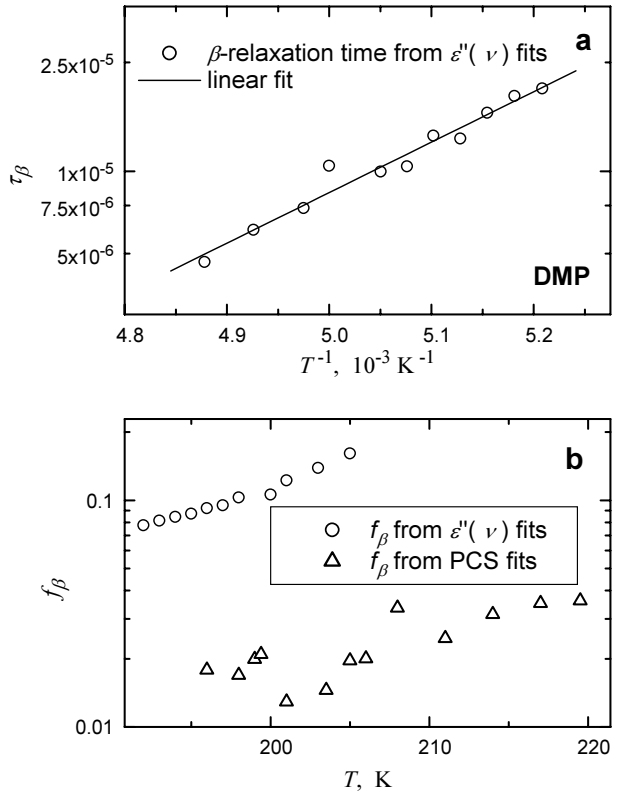

Fig. 4. Parameters of the β-relaxation of DMP versus temperature from fits to equation (12).

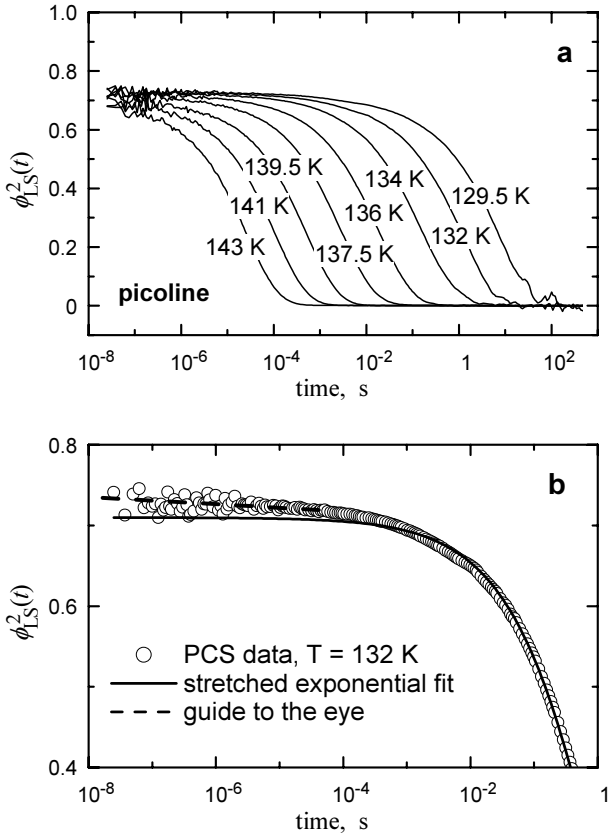

Fig. 5. (a) PCS data $\phi^2_{\rm LS}(t)$ of 2-picoline at selected temperatures. (b) Initial part of $\phi^2_{\rm LS}(t)$ at 132 K with a stretched exponential fit.

in the inset of Fig. 3a) and found that $a \approx 0.3$ and is almost temperature independent, so that it was fixed at $a = 0.3$. Figure 4 shows the β-relaxation time (a) and strength (b) versus temperature. It is seen that τ_K exhibits a typical temperature activated behavior with an activation energy of $\sim$17 kJ mol^{-1}. The strength f_β increases with temperature, which is also a characteristic feature of a β-relaxation [3]. Next we fit the photon correlation data to the same model of equation (12), where we fix the shape and relaxation time of the β-part to the values determined from the DS fits. A sample fit is shown by a short-dashed line in Figure 3a and it clearly fits the data much better than the stretched exponential alone. f_β obtained from the fits are shown in Figure 4. One observes that $f_\beta^{\rm LS}$ values are about 5 to 8 times smaller than $f_\beta^{\rm DS}$, and they show a similar temperature behavior. The last observation strongly suggests that it is indeed the same β-process observed in the LS and DS data of DMP.

Next we present PCS data of picoline in Figure 5a. The correlation functions start from $\phi_0^2 = 0.73$ on average. This value is less than $\phi_0^2 \approx 0.86$ of DMP, suggesting that the LS magnitude of the ps-dynamics of picoline $f_{fast} = 1 - \phi_0$ is about twice that of DMP. Otherwise and similar to DMP, the initial part of the correlation function exhibits observable decay beyond the main relaxation, see Figure 5b. Thus the light scattering correlation functions of picoline also reveal secondary relaxations preceeding the main α-process. In Figure 6 we compare PCS and DS data of picoline at $T \approx T_g$ in the same manner as in Figure 3 of DMP. The dielectric response of picoline is qualitatively different from that of DMP: instead of the JG β-relaxation peak of DMP, picoline exhibits an excess wing, see inset in Figure 6a. Using equation (9) with $n \approx n_D^{20\ ^\circ{\rm C}} = 1.500$ (supplier's value), we find that at 132 K the wing is strong enough to give a clearly non-KWW shape of the dielectric relaxation function, as seen from the difference between the $r^2(t)$ data and their KWW fit (dashed line). The LS correlation function (circles) also clearly deviates from its KWW fit (solid line), but again, as in the case of DMP, with much less magnitude than the dielectric data. Overall, one makes the same conclusion as with Figure 3a: the ps-dynamics of picoline are stronger in LS than in DS, while the opposite is true for the intermediate dynamics. Turning now to the frequency representation of Figure 6b, we see again a pronounced difference of the spectral shapes. In particular, LS data show no sign of the excess wing in the frequency range 1–10 kHz, whereas it is clearly displayed by the DS data. One concludes therefore that the wing feature, if present in the LS data, has to be located at higher frequencies and/or be different in shape, compared with the dielectric spectra. We attempted fitting the LS and DS data to the same model that included a wing feature and note that, even though excellent fits of the LS data were obtained, the parameters and their temperature dependence were

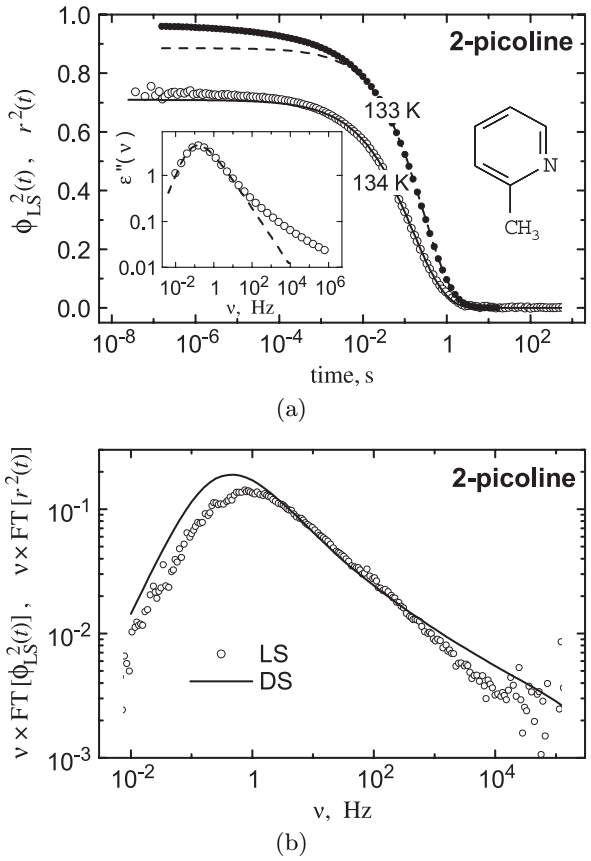

Fig. 6. (a) PCS data $\phi^2_{\rm LS}(t)$ (○) and squared normalized dielectric relaxation function $r^2(t)$ (●) of picoline at 134 K. Lines are KWW fits of $\phi^2_{\rm LS}(t)$ and $r^2(t)$ (see text for details). Inset: Dielectric loss spectrum $\epsilon''(f)$ with the same KWW fit as above. (b) $\phi^2_{\rm LS}(t)$ and $r^2(t)$ transformed into the frequency domain.

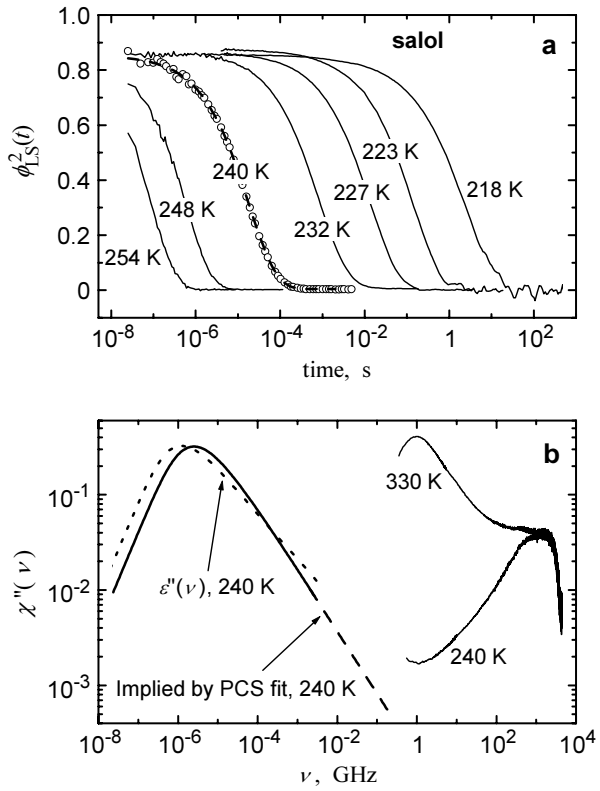

Fig. 7. (a) PCS data $\phi^2_{\rm LS}(t)$ of salol at selected temperatures. The data at 240 K (○) are shown with a KWW fit (dashed line). (b) Normalized LS susceptibility of salol at 240 and 330 K and the α-relaxation spectrum implied by the KWW fit above; short-dashed line is the dielectric loss spectrum.

not physically consistent. We take that as an additional justification of the weakness of the wing feature in light scattering.

Finally, we turn to salol and show in Figure 7 its PCS data at several selected temperatures. The dashed line in Figure 7a is an example of a KWW fit to the 240 K data. The fit for this temperature, which is about 20 K above T_g, does follow the data within the scatter, but we argue that, even at such relatively high temperature, deviations are expected at shorter (experimentally inaccessible) times. To justify this statement, we present in Figure 7b the frequency (susceptibility) spectrum of the fit along with experimental LS susceptibility spectra at 240 and 330 K in the GHz range (data from Ref. [19]). The latter are normalized, $\int_{-\infty}^{\infty} \chi''(\nu)\, d\, \ln\nu = \pi/2$. To determine the normalization factor, the experimental 330 K spectrum was extended to low frequencies, assuming $\chi''(\nu) \propto \nu$ (which is the physically correct asymptotic behavior), and integrated numerically. Then both 240 and 330 K experimental spectra were divided by the integral and multiplied by $\pi/2$. The α-relaxation susceptibility spectrum of the fit is already normalized, since it derives from a normalized correlation function. We note that the spectrum of the fit does not join up with $\chi''_{240\ \rm K}(\nu)$. More specifically, it implies much less intensity around 1 GHz than actually observed, and therefore the actual spectrum between 0.01 and 1 GHz has to have an extra contribution beyond the KWW description. We also present in the same Figure 7b a dielectric loss spectrum (shifted vertically) with the intention to show that its high frequency wing is rather different from $\chi''_{\rm KWW}(\nu)$. This observation is further substantiated below.

Figure 8 presents low-T LS and DS data of salol in the same fashion already explained for DMP and picoline. The dielectric spectrum of salol, see inset in the figure, shows a secondary relaxation feature intermediate in intensity and shape of the wing feature of picoline and the β-process of DMP. Its time domain representation strongly deviates from the stretched exponential, see the $r^2(t)$ data points and the dashed line (fit) in Figure 8a. (Temperature dependent refractive index of salol has been reported in reference [20]; we extrapolated these data to 220 K and used $n^{220\,\rm K} \approx 1.62$ in equation (9).) In contrast, the PCS data exhibit only a barely discernible deviation from their KWW fit (solid line in Figure 8a) and therefore have very little contribution of the secondary relaxation. The short-time decay of the dielectric function is thus significantly more pronounced than that of the light scattering correlation data. This is qualitatively similar to DMP and picoline. The initial values $\phi_0 = \phi_{\rm LS}(\sim 10^{-7}\,{\rm s})$

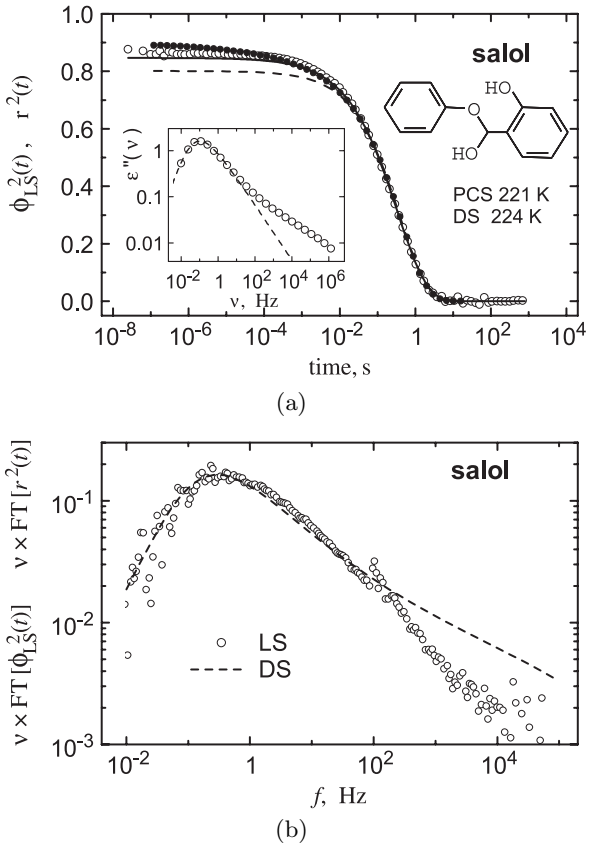

Fig. 8. (a) PCS data $\phi^2_{\rm LS}(t)$ (○) and squared normalized dielectric relaxation function $r^2(t)$ (●) of salol at $\sim T_g$. Lines are KWW fits of $\phi^2_{\rm LS}(t)$ and $r^2(t)$ (see text for details). Inset: Dielectric loss spectrum $\epsilon''(f)$ with the same KWW fit as above. (b) $\phi^2_{\rm LS}(t)$ and $r^2(t)$ transformed into the frequency domain.

and $r_0 = r(\sim 10^{-7}\,\mathrm{s})$ of salol also compare as in the other two systems, $1-\phi_0 > 1-r_0$. The frequency representation, Figure 8b, confirms that the secondary relaxation feature is almost absent from the LS spectrum, only showing up as a slight upturn at ∼10 kHz that is masked by the data scatter. Recalling the discussion of Figure 7b we note, however, that the secondary features ought to give a significant contribution to the LS spectrum at higher frequencies, and that this implies qualitatively different LS and dielectric spectral shapes. The weaknesses of the extra contribution in the PCS data precluded any further quantitative analysis.

Discussion

Summarizing, the presented comparisons of the dielectric and light scattering responses of salol, DMP, and 2-picoline reveal several features that are common for all these systems. In particular, the strength of the fast ps-dynamics is larger in the LS than in the DS data,

$$f^{\rm LS}_{fast} > f^{\rm DS}_{fast} \tag{13}$$

This can be understood following the approach of references [5,12] which, with slight modifications, leads to equations (3, 4). On the contrary, the strengths of the intermediate relaxation compare in the opposite manner,

$$f^{\rm LS}_{\beta} < f^{\rm DS}_{\beta}, \tag{14}$$

which contradicts equations (4).

In order to understand the origin of this discrepancy, we critically analyze the assumptions underlying equation (3). The absence of large angle orientational jumps was one such assumption, but we have seen that even assuming completely random angle jumps does not lead to $1-\phi_2(t) < 1-\phi_1(t)$. However, the situation will be different for a process that involves 180° jumps. Indeed, reorientations by 180° do not cause decay of $\phi_2(t)$ and therefore do not contribute to the corresponding spectrum. Schilling et al. report a MD study of a liquid of linear molecules in which they observed frequent 180° jumps [21]. They conclude that the marked difference between their $\phi_2(t)$ and $\phi_1(t)$ is a consequence of these jump processes [22]. It is however unlikely that 180° jumps are statistically significant events in real molecular glass-formers, which usually lack the C_2 molecular symmetry. Indeed, Sindzingre and Klein report on a MD study of methanol [23] where they did observe jump reorientations, but they were not 180° flips. Moreover, it is rather unlikely that occasional jumps of individual molecules give significant contribution on the timescale of intermediate relaxations. Concluding, it is therefore unlikely that large angle jumps can explain the differences that we observe for the β-relaxation.

A somewhat related consideration follows from the observation that flat molecules are likely to have approximately axisymmetric polarizability with the principal axis orthogonal to the molecular plane, while the molecular dipole, if any, will lie in the plane. Then, anisotropic processes that correspond to reorientations in the plane will be manifested in the DS response and almost absent from the LS one. Salol and picoline are examples of such molecules, and one can therefore argue that their secondary relaxations are related to anisotropic in-plane reorientations and thus weakly pronounced in the LS spectra. This explanation however does not hold for DMP, which is neither a flat, nor a rigid molecule. Moreover, NMR lineshapes of several molecular glassformers, including toluene that is structurally very similar to picoline, are consistent with the assumption that, close to T_g, there is no preferred axis for molecular reorientations [24]. However, other authors conclude from NMR spin-lattice relaxation time analyses that the rotational motions corresponding to the β-process of toluene at and below T_g are anisotropic [25]. We therefore tentatively note that the weakness of the LS secondary relaxations of salol and picoline may be a result of anisotropic, mostly in-plane, character of their secondary reorientational dynamics.

We now recall that we neglected interaction-induced contributions, such as DID (Dipole Induced Dipole), to the dielectric and polarizability fluctuations. In dielectric spectroscopy, one can argue that, if the molecules possess large permanent dipole moments, then the single-molecule (allowed) spectral contribution is much stronger than the (second order) interaction-induced ones and therefore the

latter are likely negligible in the dielectric response. Their possible contributions to LS spectra have been subject to much controversy in the literature. In the case of significantly anisotropic molecules one can use the same argument as above to conclude that interaction-induced effects are relatively small, but such reasoning is not completely satisfactory. Existing experimental evidence seems however to indicate that they are indeed negligible in the case of relatively large and anisotropic molecules, such as salol [26]. It therefore appears unlikely that interaction-induced effects are strongly pronounced in our data. Yet we would like to point out that, in the spectral range of secondary relaxations, the spectral density is rather weak. It is thus entirely possible that even weakly allowed second order contributions may significantly alter its spectral shape. One further notes that the DID mechanism, by virtue of the properties of the dipole field that makes the induced dipole magnitude very sensitive to interparticle distances, effectively reveals density fluctuations that do not directly couple to the electric polarization or anisotropic polarizability and therefore are not otherwise visible in DS and depolarized LS spectra. Moreover, the whole **q**-space is mapped onto the (low) **q** of observation. If, as suggested by Arbe et al. [27], the secondary relaxations are primarily manifested in the density fluctuation dynamics at relatively high **q**, then their manifestation in low-**q** spectra, such as our LS and DS data, is only possible through second order effects that may be rather different in the LS and DS responses.

Finally, it is quite obvious that molecular reorientations in a dense liquid are strongly correlated on short scales, and therefore intermolecular contributions to the correlation functions and corresponding spectra cannot be ignored. These contributions will likely be different for LS and DS spectra.

In conclusion, we have experimentally detected "slow" secondary relaxation features in depolarized light scattering of three simple molecular liquids, dimethylphthalate, 2-picoline, and salol. We have found that the magnitude of these features is invariably much smaller than in the corresponding dielectric response. We were unable to find a single general explanation of this difference and note that it may be just an accidental property of the systems that we chose. Further investigations are therefore needed.

Indispensable assistance of Jürgen Gmeiner and Irene Bauer (Bayreuth University) in sample preparation is gratefully acknowledged. Stimulating discussions with Per Jacobsson and Lars Börjesson (Chalmers University) are deeply appreciated.

References

1. W. Götze, L. Sjögren, Rep. Prog. Phys **55**, 241 (1992)
2. G. Johari, M. Goldstein, J. Chem. Phys. **53**, 2372 (1970)
3. A. Kudlik, S. Benkhof, T. Blochowicz, C. Tschirwitz, E. Rössler, J. Molec. Struct. **479**, 201 (1999)
4. S.V. Adichtchev, St. Benkhof, Th. Blochowicz, V.N. Novikov, E. Rössler, Ch. Tschirwitz, J. Wiedersich, Phys. Rev. Lett. **88**, 055703-1 (2002)
5. T. Blochowicz, A. Kudlik, S. Benkhof, J. Senker, E. Rössler, G.Hinze, J. Chem. Phys **110**, 12011 (1999)
6. B.J. Berne, R. Pecora, *Dynamic Light Scattering* (Wiley, New York, 1976)
7. G. Fytas, Macromolecules **22**, 211 (1989)
8. G.D. Patterson, P.K. Jue, D.J. Ramsay, J.R. Stevens, J. Polym. Sci. B **32**, 1137 (1994)
9. R. Bergman, L. Börjesson, L.M. Torell, A. Fontana, Phys. Rev. B **56**, 11619 (1997)
10. D. Sidebottom, R. Bergman, L. Börjesson, L.M. Torell, Phys. Rev. Lett. **71**, 2260 (1993)
11. L. Comez, D. Fioretto, L. Palmieri, L. Verdini, P.A. Rolla, J. Gapinski, T. Pakula, A. Patkowski, W. Steffen, E.W. Fischer, Phys. Rev. E **60**, 3086 (1999)
12. M.J. Lebon, C. Dreyfus, Y. Guissani, R.M. Pick, H.Z. Cummins, Z. Phys. B **103**, 433 (1997)
13. E.N. Ivanov, Sov. Phys. JETP **18**, 1041 (1964)
14. S.K. Nayak, S.S.N. Murthy, J. Chem. Phys. **99**, 1607 (1993)
15. S. Benkhof, Diplomarbeit, Universität Bayreuth (1995)
16. A. Kudlik, S. Benkhof, R. Lenk, E. Rössler, Europhys. Lett. **32**, 511 (1995)
17. C.J.F. Böttcher, P. Bordewijk, *Theory of Electric Polarization* (Elsevier, Amsterdam, 1978)
18. T. Blochowicz, Ch. Tschirwitz, St. Benkhof, E.A. Rössler, J. Chem. Phys **118**, 7544 (2003)
19. A. Brodin, H.Z. Cummins, H. Zhang, unpublished data
20. G.D. Enright, B.P. Stoicheff, J. Chem. Phys. **64**, 3658 (1976)
21. S. Kämmerer, W. Kob, R. Schilling, Phys. Rev. E **56**, 5450 (1997)
22. S. Kämmerer, W. Kob, R. Schilling, Phys. Rev. E **58**, 2141 (1998)
23. P. Sindzingre, M. Klein, J. Chem. Phys. **96**, 4681 (1992)
24. M. Vogel, E. Rössler, J. Chem. Phys **115**, 10883 (2001)
25. G. Hinze, H. Sillescu, F. Fujara, Chem. Phys. Lett. **232**, 154 (1995)
26. H.Z. Cummins, G. Li, W. Du, R.M. Pick, C. Dreyfus, Phys. Rev. E **53**, 896 (1996)
27. A. Arbe, D. Richter, J. Colmenero, B. Farago, Phys. Rev. E **54**, 3853 (1996)